

High speed InAs electron avalanche photodiodes overcome the conventional gain-bandwidth product limit

Andrew R. J. Marshall,^{1,*} Pin Jern Ker,² Andrey Krysa,² John P. R. David,²
and Chee Hing Tan²

¹Physics Department, Lancaster University, Lancaster, LA1 4YB, UK

²Department of Electronic and Electrical Engineering, University of Sheffield, Sir Frederick Mappin Building,
Mappin Street, Sheffield, S1 3JD, UK
a.r.marshall@lancaster.ac.uk

Abstract: High bandwidth, uncooled, Indium Arsenide (InAs) electron avalanche photodiodes (e-APDs) with unique and highly desirable characteristics are reported. The e-APDs exhibit a 3dB bandwidth of 3.5 GHz which, unlike that of conventional APDs, is shown not to reduce with increasing avalanche gain. Hence these InAs e-APDs demonstrate a characteristic of theoretically ideal electron only APDs, the absence of a gain-bandwidth product limit. This is important because gain-bandwidth products restrict the maximum exploitable gain in all conventional high bandwidth APDs. Non-limiting gain-bandwidth products up to 580 GHz have been measured on these first high bandwidth e-APDs.

©2011 Optical Society of America

OCIS codes: (040.1345) Avalanche photodiodes (APDs); (250.0040) Detectors

References and links

1. R. J. McIntyre, "Multiplication noise in uniform avalanche diodes," *IEEE Trans. Electron. Dev.* **13**(1), 164–168 (1966).
2. R. B. Emmons, "Avalanche-photodiode frequency response," *J. Appl. Phys.* **38**(9), 3705–3714 (1967).
3. B. E. A. Saleh, M. M. Hayat, and M. C. Teich, "Effect of dead space on the excess noise factor and time response of avalanche photodiodes," *IEEE Trans. Electron. Dev.* **37**(9), 1976–1984 (1990).
4. J. D. Beck, C.-F. Wan, M. A. Kinch, and J. E. Robinson, "MWIR HgCdTe avalanche photodiodes," *Proc. SPIE* **4454**, 188–197 (2001).
5. J. Beck, C. Wan, M. Kinch, J. Robinson, P. Mitra, R. Scritchfield, F. Ma, and J. Campbell, "The HgCdTe electron avalanche photodiode," *J. Electron. Mater.* **35**(6), 1166–1173 (2006).
6. J. Rothman, G. Perrais, G. Destefanis, J. Baylet, P. Castelein, and J.-P. Chamonal, "High performance characteristics in pin MW HgCdTe e-APDs," *Proc. SPIE* 6542, 654219, 654219-10 (2007).
7. F. Ma, X. Li, J. Campbell, J. Beck, C.-F. Wan, and M. A. Kinch, "Monte Carlo simulations of Hg_{0.7}Cd_{0.3}Te avalanche photodiodes and resonance phenomenon in the multiplication noise," *Appl. Phys. Lett.* **83**(4), 785–787 (2003).
8. A. R. J. Marshall, C. H. Tan, M. J. Steer, and J. P. R. David, "Electron dominated impact ionization and avalanche gain characteristics in InAs photodiodes," *Appl. Phys. Lett.* **93**(11), 111107 (2008).
9. A. R. J. Marshall, C. H. Tan, M. J. Steer, and J. P. R. David, "Extremely low excess noise in InAs electron avalanche photodiodes," *IEEE Photon. Technol. Lett.* **21**(13), 866–868 (2009).
10. A. R. J. Marshall, J. P. R. David, and C. H. Tan, "Impact ionization in InAs electron avalanche photodiodes," *IEEE Trans. Electron. Dev.* **57**(10), 2631–2638 (2010).
11. A. R. J. Marshall, P. Vines, P. J. Ker, J. P. R. David, and C. H. Tan, "Avalanche multiplication and excess noise in InAs electron avalanche photodiodes at 77K," *IEEE J. Quantum Electron.* **47**(6), 858–864 (2011).
12. G. Perrais, J. Rothman, G. Destefanis, and J.-P. Chamonal, "Impulse response time measurements in Hg_{0.7}Cd_{0.3}Te MWIR avalanche photodiodes," *J. Electron. Mater.* **37**(9), 1261–1273 (2008).
13. C. H. Tan, J. S. Ng, S. Xie, and J. P. R. David, "Potential materials for avalanche photodiodes operating above 10Gb/s," 2009 International Conference on Computers and Devices for Communication, 2009.
14. J. C. Campbell, S. Demiguel, F. Ma, A. Beck, X. Guo, S. Wang, X. Zheng, X. Li, J. D. Beck, M. A. Kinch, A. Huntington, L. A. Coldren, J. Decobert, and N. Tschertner, "Recent advances in avalanche photodiodes," *IEEE J. Sel. Top. Quantum Electron.* **10**(4), 777–787 (2004).
15. K. Kiasaleh, "Performance of APD-based, PPM free-space optical communication systems in atmospheric turbulence," *IEEE Trans. Commun.* **53**(9), 1455–1461 (2005).
16. J. C. Campbell, W. T. Tsang, G. J. Qua, and B. C. Johnson, "High-speed InP/InGaAsP/InGaAs avalanche photodiodes grown by chemical beam epitaxy," *IEEE J. Quantum Electron.* **24**(3), 496–500 (1988).

17. W. R. Clark, A. Margittai, J.-P. Noel, S. Jatar, H. Kim, E. Jamroz, G. Knight, and D. Thomas, "Reliable, high gain-bandwidth product InGaAs/InP avalanche photodiodes for 10Gb/s receivers," Proc. OFC/IOOC, 96–98 (1999).
18. T. Nakata, T. Takeuchi, I. Watanabe, K. Makita, and T. Torikai, "10Gbit/s high sensitivity, low-voltage-operation avalanche photodiodes with thin InAlAs multiplication layer and waveguide structure," Electron. Lett. **36**, 2033–2034 (2000).
19. M. Lahrchi, G. Glastre, E. Derouin, D. Carpentier, N. Lagay, J. Decobert, and M. Achouche, "240-GHz Gain-bandwidth product back-side illuminated AlInAs avalanche photodiodes," IEEE Photon. Technol. Lett. **22**(18), 1373–1375 (2010).
20. C. Lenox, H. Nie, P. Yuan, G. Kinsey, A. L. Homles, B. G. Streetman, and J. C. Campbell, "Resonant-cavity InGaAs-InAlAs avalanche photodiodes with gain-bandwidth product of 290GHz," IEEE Photon. Technol. Lett. **11**(9), 1162–1164 (1999).
21. G. S. Kinsey, J. C. Campbell, and A. G. Dentai, "Waveguide avalanche photodiode operating at 1.55 μ m with a gain-bandwidth product of 320GHz," IEEE Photon. Technol. Lett. **13**(8), 842–844 (2001).
22. S. Assefa, F. Xia, and Y. A. Vlasov, "Reinventing germanium avalanche photodetector for nanophotonic on-chip optical interconnects," Nature **464**(7285), 80–84 (2010).
23. Y. Kang, H.-D. Liu, M. Morse, M. Paniccia, M. Zadka, Y. Kang, H.-D. Liu, M. Morse, M. J. Paniccia, M. Zadka, S. Litski, G. Sarid, A. Pauchard, Y.-H. Kuo, H.-W. Chen, W. S. Zaoui, J. E. Bowers, A. Beling, D. C. McIntosh, X. Zheng, and J. C. Campbell, "Monolithic germanium / silicon avalanche photodiodes with 340GHz gain-bandwidth product," Nat. Photonics **3**(1), 59–63 (2009).
24. W. S. Zaoui, H.-W. Chen, J. E. Bowers, Y. Kang, M. Morse, M. J. Paniccia, A. Pauchard, and J. C. Campbell, "Frequency response and bandwidth enhancement in Ge/Si avalanche photodiodes with over 840 GHz gain-bandwidth-product," Opt. Express **17**(15), 12641–12649 (2009).
25. A. R. J. Marshall, C. H. Tan, J. P. R. David, J. S. Ng, and M. Hopkinson, "Fabrication of InAs photodiodes with reduced surface leakage current," Proc. SPIE 6740, 67400H, 67400H-9 (2007).
26. P. J. Ker, A. R. J. Marshall, A. B. Krysa, J. P. R. David, and C. H. Tan, "Temperature dependence of leakage current in InAs avalanche photodiodes," IEEE J. Quantum Electron. **47**(8), 1123–1128 (2011).
27. J.-W. Shi, F.-M. Kuo, and B.-R. Huang, "Zn-Diffusion InAs photodiodes on semi-insulating GaAs substrate for high speed and low dark current performance," IEEE Photon. Technol. Lett. **23**(2), 100–102 (2011).
28. G. Satyanadh, R. P. Joshi, N. Abedin, and U. Singh, "Monte Carlo calculation of electron drift characteristics and avalanche noise in bulk InAs," J. Appl. Phys. **91**(3), 1331–1338 (2002).
29. P. Hill, J. Schlafer, W. Powazinik, M. Urban, E. Eichen, and R. Olshansky, "Measurement of hole velocity in n-type InGaAs," Appl. Phys. Lett. **50**(18), 1260–1262 (1987).

1. Introduction

In recent years a new class of avalanche photodiode (APD) has emerged, the electron avalanche photodiode (e-APD), which embodies practically many characteristics of a theoretically ideal APD. Since early theoretical works by McIntyre [1] and Emmons [2] it has been understood that an ideal APD should derive its gain from the impact ionization of only one carrier type. In this case the ratio (k) of the ionization coefficients for electrons (α) and holes (β) becomes zero. Although either $\alpha = 0$ or $\beta = 0$ could give the $k = 0$ condition, to date only APDs where $\beta = 0$ have been demonstrated. These APDs are referred to as e-APDs, due to their avalanche multiplication being entirely derived from the impact ionization of electrons.

Compared with all conventional APDs, three key advantages are expected for true e-APDs, resulting from their unique feedback-free avalanche multiplication process. Firstly high linear mode gains are more exploitable since their gain rises exponentially with increasing electric field, instead of undergoing a classical abrupt breakdown. Secondly their excess noise factor (F) is minimized to closely approaching that of a photomultiplier tube and always remains below 2 [3]. Indeed if the ionization deadspace becomes large with respect to the mean ionization path length, α^{-1} , F can even approach the ultimate limit of unity. Thirdly the maximum impulse response duration for an e-APD will remain constant irrespective of its operational gain, being equal to the sum of the electron and hole transit times across the multiplication region. Hence, unlike all other APDs, e-APDs should never be restricted by a gain-bandwidth product limit.

Electron APDs have recently been demonstrated in the II-VI and III-V material systems, using HgCdTe [4–7] and InAs [8–11] respectively, and their defining gain and excess noise characteristics are now established in practice as well as theory. Furthermore recent work on Hg_{0.7}Cd_{0.3}Te e-APDs has led to the demonstration that e-APDs can support gain-bandwidth products as high as 1 THz [12]. However the bandwidth of these Hg_{0.7}Cd_{0.3}Te e-APDs is

limited to hundreds of MHz and due to their low bandgap energy they are operated at 77 K. In this work we report high bandwidth InAs e-APDs, which can be operated at room temperature and exploit the unique characteristics of e-APDs to demonstrate record gain-bandwidth products, for high bandwidth APDs.

The ability to support high gain-bandwidth products is becoming increasingly important for APDs used in optical communications. As channel bandwidths rise, conventional APDs increasingly fail to provide the desired signal gain without becoming gain-bandwidth limited [13,14]. As evident in Fig. 1, the optimum modeled sensitivity of a typical 10 Gbps receiver is achieved with an APD gain >10 even when $k = 1$, and increases as k reduces towards zero. The estimated APD gain-bandwidth products required to closely approach these optimum sensitivities in practice exceed the gain-bandwidth product limits of established APDs. Hence it is evident that gain-bandwidth product limits are already restricting the optimum sensitivity achievable in 10 Gbps APD receivers. This restriction will only be exacerbated by a move to 40 Gbps, where gain-bandwidth products as high as 1 THz or more become desirable. The restriction imposed by the gain-bandwidth product limit is also particularly relevant for terrestrial or satellite free space optical links, where the ability to exploit high APD gains maximizes the link's fade margin [15]. Furthermore APDs supporting high gains at high bandwidth can also enable high sensitivity, time resolved, scientific and imaging applications.

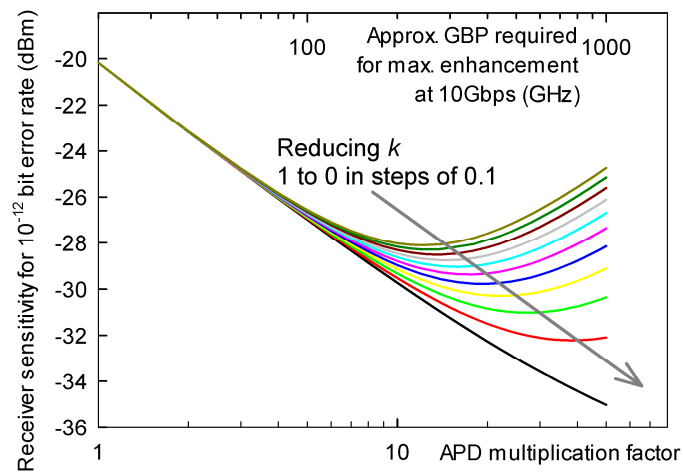


Fig. 1. The modelled receiver sensitivity for a 10 Gbps APD receiver, excluding gain-bandwidth product limits, taking the input referenced amplifier noise to be $14 \text{ pAHz}^{1/2}$. The upper x-axis shows the estimated APD gain-bandwidth product (GBP), in GHz, required to closely approach the modelled sensitivity enhancement in practice.

Emmons [2] provided an expression which describes the way in which an APD's gain-bandwidth product limit varies, as a function of the multiplication region width (w) and k . A contour plot representation of this is shown in Fig. 2 to illustrate the expected trends. To-date the development of high bandwidth APDs has focused on reducing w to as little as 100 nm [16–21], while k has typically remained ≥ 0.2 . The gain-bandwidth products reported for such devices and other state-of-the-art high bandwidth APDs, are shown in Fig. 2. There is limited potential for pursuing the trend of reducing w further because tunneling imposes a practical lower limit. Indeed one of the highest gain-bandwidth products reported to date, was for a novel Germanium APD [22] in which the high electric field was highly localized, however the concomitant penalty appears to have been very high leakage current. Figure 2 illustrates that there is significant potential for increasing gain-bandwidth products by reducing k . Kang *et al.* [23] exploited this approach, using a silicon multiplication region with $k \sim 0.08$ to achieve a record gain-bandwidth product limit for high bandwidth APDs, despite their APD having a much larger w than state-of-the-art III-V APDs. Further characterization of these devices by Zaoui *et al.* [24] under higher biases showed that nonlocal effects can increase the bandwidth

measurements at 77K indicated a minimum background doping in the *n-i-p* diodes of $5\text{-}7 \times 10^{14}$ atoms/cm³ across the central 4 μm , which depleted under 5 V reverse bias. Beyond this cladding dopant diffusion increased the doping concentration and reduced the rate of depletion, with 5 μm depleted at 12 V.

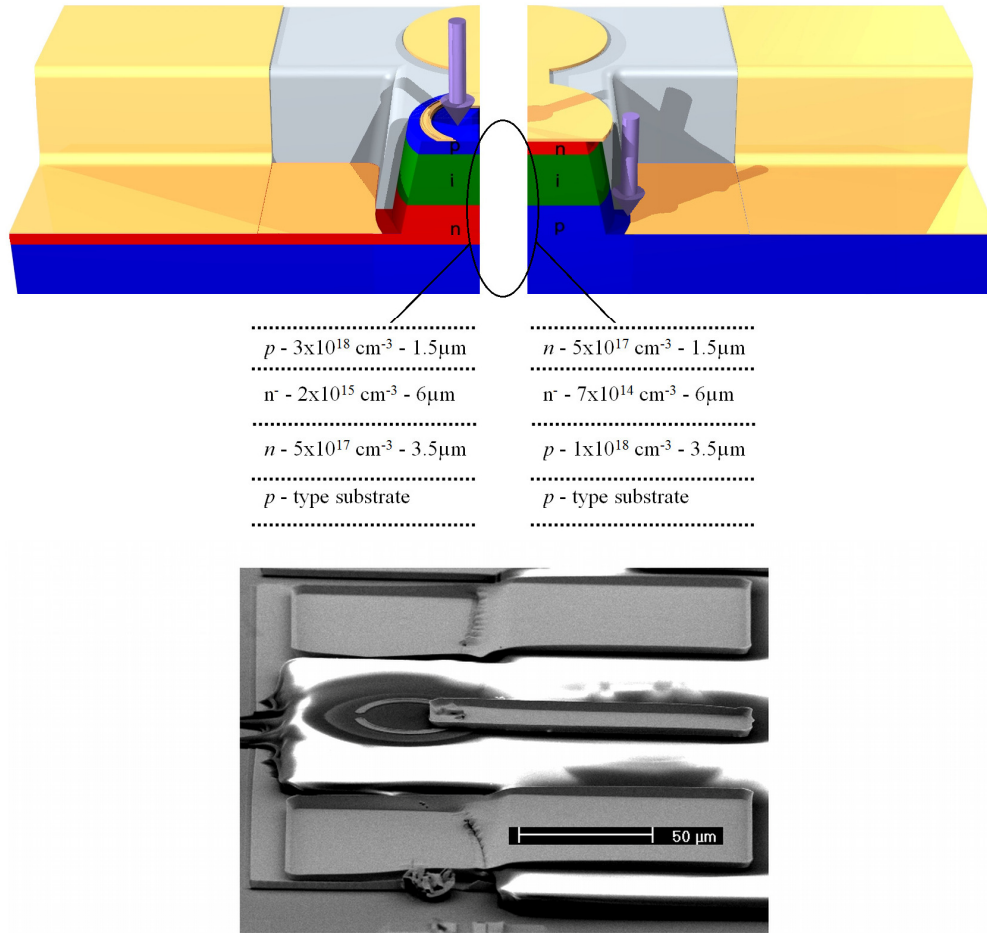


Fig. 3. A schematic cross section view of our *p-i-n* and *n-i-p* e-APD structures showing the different top contact designs employed to aid characterization, with SU-8 passivation (cut away) and the epilayer details. The areas illuminated are indicated with arrows. Also shown is an SEM image of a fully fabricated *p-i-n* e-APD.

Mesa diodes with nominal diameters after etching of 35 μm , 60 μm , 85 μm , 135 μm and 235 μm were defined using wet chemical etching routines similar to those described elsewhere [25]. The mesa sidewalls were encapsulated and passivated with SU-8 immediately after etching, in order to both minimise the reverse leakage current and act as an insulating dielectric for the remote ground-signal-ground pads. Ti/Pt/Au, 10/20/200 nm, and Ti/Au, 25/200 nm, were used for *p*-type and *n*-type contacts respectively, which were then contacted by Ti/Au ground-signal-ground pads. Without contact annealing the 35 μm diameter devices had a typical series resistance of 105 Ω , however this is significantly higher than usually achieved for InAs e-APDs. A series resistance of 10-15 Ω is more typical for such InAs e-APDs without remote contact pads; hence the increased resistance seen in these high bandwidth devices is attributed to the prototype remote contacted structure and fabrication scheme.

To ensure the best performance from e-APDs, all primary photocurrent should originate from the p-type cladding, with only photogenerated electrons entering the region of higher electric field. To achieve this with the *n-i-p* diodes a metal cap was applied to shadow the n-type cladding and light was focused next-to the mesa, as shown in Fig. 3. Due to the long minority electron diffusion length in InAs this is analogous to removing the substrate and using backside illumination. For *p-i-n* diodes focused illumination on the mesa top provided the desired primary photocurrent. Photomultiplication measurements were performed using a modulated 1462 nm laser source and a lock-in amplifier to provide phase sensitive detection of the photocurrent. This technique was employed to ensure that the avalanche gain was determined accurately in the presence of leakage currents, which were in some cases of comparable or greater magnitude. To measure the frequency response of the e-APDs, radio frequency (RF) optical signals were generated using a 1310 nm laser and a modulating RF source. The light was coupled into the diodes via a single mode fiber at room temperature and a multimode fiber at 77 K. A 50 GHz ground-signal-ground probe was used to contact to the diode under test and the RF photocurrent was passed back to a microwave transition analyzer using appropriate cabling and a bias-tee, through which the reverse bias was applied to the device under test. The loss within the cabling, connectors and bias-tee was calibrated across the measurement frequency range using a vector network analyzer. The supplier's calibration data was used to account for loss in the ground-signal-ground probe. Characterization at 77 K was performed in a low vibration, liquid nitrogen cooled, micro-manipulated probe-station.

3. Results and discussion

The external quantum efficiency of the *p-i-n* e-APDs under top side illumination was measured to be 51% at 1.55 μm , without anti-reflection coating. With this wavelength essentially all the primary photocurrent was generated in the undepleted p-type cladding, as required to obtain the optimum performance from such *p-i-n* e-APDs. In this case the external quantum efficiency was limited by recombination of the minority photogenerated electrons within this cladding. Modifications to the cladding structure and improvements in the material quality could increase the proportion of photogenerated electrons diffusing to the intrinsic region and hence also the quantum efficiency. Although this would be desirable, it is noted that the simple addition of an anti-reflection coating could increase the external quantum efficiency of the current e-APDs to approximately 70%, which is already competitive. Figure 4 shows the measured leakage current, photocurrent and multiplication.

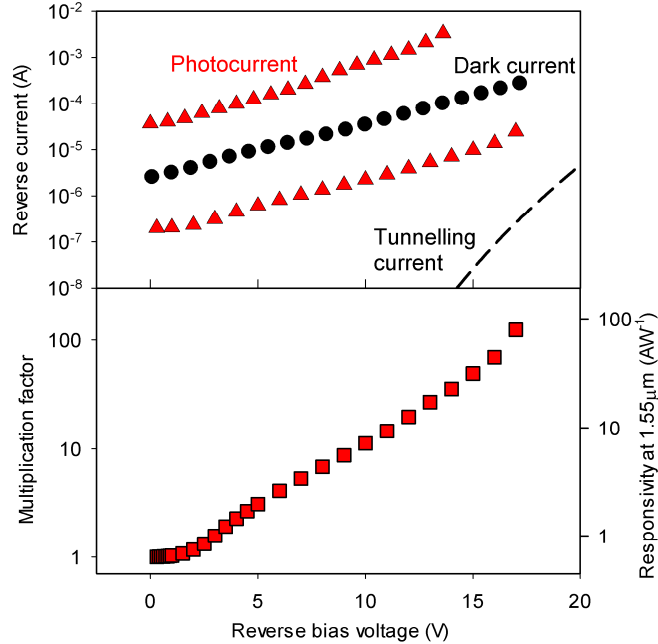


Fig. 4. Measured leakage and photocurrents at room temperature, together with the modelled tunnelling current and the corresponding measured multiplication and calculated responsivity.

It has only recently become possible to realize high bandwidth InAs e-APDs with the identification of a suitable dielectric which could be used without triggering excessive surface leakage [26]. Another key enabling technology has been metal organic vapor phase epitaxial growth of thick, high quality InAs layers with low background doping concentrations. Uniquely in InAs e-APDs, the multiplication factor achieved for a given reverse bias voltage increases with increasing depletion width [8]. This characteristic has been exploited here to achieve high multiplication without excessive tunneling currents, despite the low bandgap energy. Although the leakage in these InAs e-APDs at room temperature is higher than in established wider bandgap APD technologies, it is comparable with other novel technologies for which the highest gain-bandwidth products have been reported [22,23], as shown in Fig. 5. As the technology matures, further reductions in leakage current should be realized through improvements in crystal quality and surface passivation.

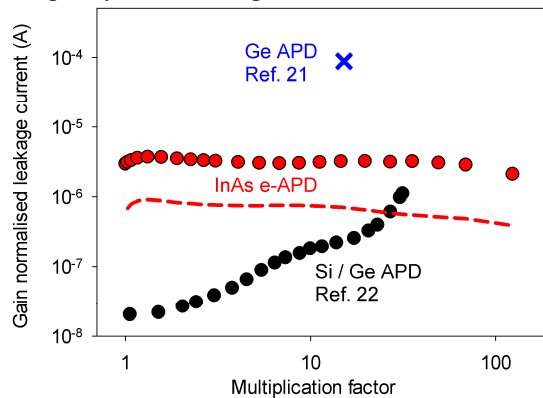


Fig. 5. Comparison of the gain normalized leakage current in our InAs e-APDs with other recently reported small area high gain-bandwidth APDs. Also shown is the expected gain normalized leakage current in a 25 μ m diameter InAs e-APD in the absence of surface leakage (---), calculated from fitting to the measured leakage current in larger diodes.

The frequency responses of different area diodes and the multiplication dependence of the bandwidth, are shown in Fig. 6. The measured 3dB bandwidths for the largest, 235 μm and 135 μm diameter e-APDs can be fitted based on RC considerations, however as noted earlier the series resistances of these prototype high speed APDs were found to be atypically high for InAs e-APDs. In comparison the 3 dB bandwidths of smaller devices cannot be fitted based on RC or transit time considerations. Furthermore the results have proven insensitive to variations in the signal track design, indicating that the capacitance between it and the conducting substrate is not the limiting factor. Instead other parasitic effects associated with the conducting substrate and dielectric are considered to limit the maximum bandwidth of our e-APDs to 3.5 – 4 GHz. Employing a semi-insulating substrate, as recently reported for high bandwidth unity gain InAs photodiodes [27], would increase the maximum bandwidths. Despite having large depletion widths the InAs e-APDs' bandwidths are not build-up or transit time limited because of the absence of feedback in the avalanche multiplication and the commensurate two carrier transit time limit on the impulse response.

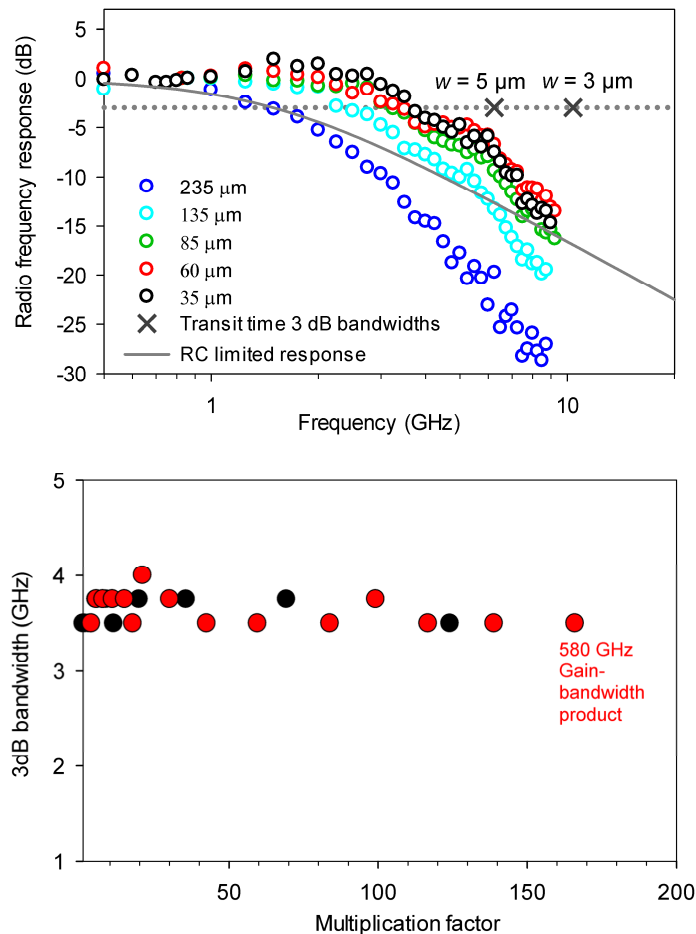


Fig. 6. (Top) Frequency responses measured at room temperature on *n-i-p* InAs e-APDs of different diameters (see key), operating at a gain of 11.3 (10 V reverse bias). Also shown are the transit time limited 3 dB bandwidths modelled for multiplication region widths of 5 μm and 3 μm (x), using the saturated drift velocities reported for electrons in InAs [28] and holes in InGaAs [29] and the modelled RC frequency response for the 235 μm diameter e-APDs based on measured values of R and C. (Bottom) The measured 3 dB bandwidth of InAs *n-i-p* e-APDs as a function of device gain, at room temperature (●) and 77 K (●).

One undesirable side effect of the trend towards thinner multiplication widths in conventional high bandwidth APDs has been the commensurate increase in capacitance / unit area. To avoid this limiting the bandwidth, device areas have been progressively reduced. In contrast the wide depletion widths and low series resistances, characteristic of InAs e-APDs, uniquely allow large area diodes to operate at high bandwidths. This could be highly advantageous in non-fibre based imaging and sensing applications.

The gain dependence of the measured 3 dB bandwidth, as shown in Fig. 6, is strikingly lacking in the usual high gain roll-off, instead the bandwidth remains essentially constant for all gains. Although expected for e-APDs, this has not been demonstrated in practice before in a high bandwidth APD. Unrestricted by gain-bandwidth product limits which afflict conventional APDs with non-zero values of k , our InAs e-APDs have reached gain-bandwidth products of 430 GHz at room temperature and 580 GHz at 77 K where higher stable gains can be achieved at this time.

4. Conclusion

In this work high bandwidth InAs e-APDs have been designed and fabricated. In line with expectations for theoretically ideal APDs, their bandwidths have been shown to remain essentially constant at all gains. Gain-bandwidth products up to 580 GHz have been achieved to-date, however this value was only limited by the maximum stable gain in these prototypes. As InAs e-APD technology matures higher bandwidths and stable gains are expected as are gain-bandwidth products greater than 1 THz. In contrast gain-bandwidth product limits for conventional APDs already approach or meet the limits imposed by material constants. Finally with cooled operation, InAs e-APDs could even approaching single photon detection at GHz bandwidths, enabled by their unique ability to amplify highly without suffering a reduction in bandwidth or the conventional single photon APD breakdown event, which requires a bandwidth limiting quench.

Acknowledgements

The work reported in this paper was principally funded by the Electro-Magnetic Remote Sensing Defence Technology Centre, established by the UK Ministry of Defence. Further funding has been received from the EPSRC under grant EP/H031464/1. A. Marshall is supported by a Royal Academy of Engineering research fellowship. The authors would like to thank James Green for useful discussion and assistance with figure preparation.